Performance Assessment of the VSC Using Two Model Predictive Control Schemes

Al hasheem, Mohamed; Abdelhakim, Ahmed; Dragicevic, Tomislav; Dalessandro, Luca; Blaabjerg, Frede

Published in:
Proceedings of 2018 IEEE Applied Power Electronics Conference and Exposition (APEC)

DOI (link to publication from Publisher):
10.1109/APEC.2018.8341050

Publication date:
2018

Document Version
Accepted author manuscript, peer reviewed version

Performance Assessment of the VSC Using Two Model Predictive Control Schemes

M. Alhasheem[1,2], A. Abdelhakim[3], T. Dragicevic[1], L. Dalessandro[4] and F. Blaabjerg[1]
[1]Department of Energy Technology, Aalborg University, Aalborg, Denmark
[2]Arab Acadmey for Science, Technology and Maritime Transport, Cairo, Egypt
[3] Department of Management and Engineering, University of Padova, Vicenza, Italy
[4]Schaffner Group, Luterbach, Switzerland
E-mail: mah@et.aau.dk, ahmed.a.abdelrazek@ieee.org, tdr@et.aau.dk,
luca.dalessandro@schaffner.com, fbl@et.aau.dk

***Abstract*—Finite control set model predictive control (FCS-MPC) methods in different power electronics application are gaining high attention due to their simplicity and fast dynamics. This paper introduces an experimental assessment of the two-level three-phase voltage source converter (2L-VSC) using two FCS-MPC algorithms. In order to perform such comparative evaluation, the 2L-VSC efficiency and total harmonics distortion voltage (THDv) have been measured where considering a linear load and non-linear load. The new algorithm gives better results than the conventional algorithm in terms of the THD and 2L-VSC efficiency. The results also demonstrate the performance of the system using carrier based pulse width modulation (CB-PWM). These findings have been validated for both linear and non-linear loads through experimental verification on 4 kW 2L-VSC prototype. It can be concluded that a comparable performance is achieved by using the conventional FCS-MPC, Improved FCS-MPC, and CB-PWM algorithms.**

I. Introduction

Power electronic converters are the most relevant part in any power conditioning stage, which is used to fulfil the different load requirements, either in grid connected mode [1–5] or in islanded mode [6]. Hence, it is of paramount importance to optimize their operation. Such optimization can be accomplished through several control methods such as, deadbeat control [7], cascaded linear control [8, 9], and the fuzzy control [10]. However, these methods introduce several design considerations in order to achieve a suitable control method due to digital implementation and also non linearities. Recently, MPC has been successfully implemented with existing control platform. Accordingly, predictive control has been applied to the power electronic converters due to its robust tracking ability of the references and fast dynamic response during the steady state and transient operation [11, 12]. Under an MPC scheme, the 2L-VSC can be modelled as a system with finite number of switching states, where a cost function (CF) can be evaluated for each state. Then the switching state that gives the minimum value of the CF is applied. Different formulations of the CF can be utilized as discussed in [6]. Fig. 1 shows a 2L-VSC used in this work, which is applying the conventional algorithm [6] and also the new improved algorithm as proposed in [13]. The conventional algorithm uses the measured output voltage in order to predict the future behaviour of the system, where the improved algorithm uses the voltage and its derivative in order to predict the future behaviour. In order to reduce the conversion time required by the control platform, a current estimator is used in this work. Therefore, two schemes are considered to apply the predictive algorithms. The first scheme uses all the measurements of the system, while the second scheme uses an observer to estimate the load current. The reason for operating both schemes is to validate the behaviour of the observer and involve it in the future work. On the other hand, the CB-PWM is a basic energy processing technique applied in power converter system. The PWM converter should meet some general demands, such as the wide range of linear operation and minimal number of switchings to maintain low switching losses in the power components [14]. In this paper, a CB-PWM technique, as shown in Fig. 2, is used to control the 2L-VSC in order to asses its performance compared to the predictive control algorithms. Comparing the two FCS-MPC algorithms to the CB-PWM in terms of efficiency gives a classification to the performance of the FCS-MPC.

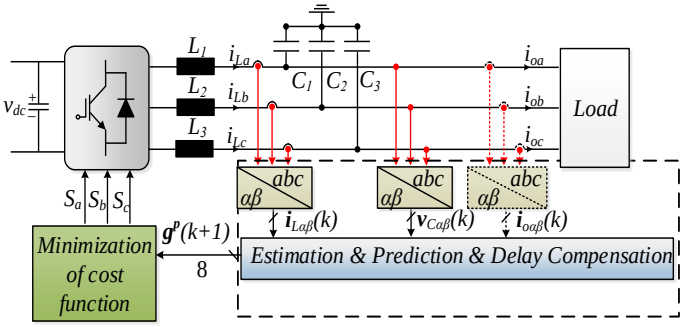

Fig. 1. General structure of the predicive control for a voltage source converter (VSC) with an output LC filter.

This paper includes the following sections; Section II presents the model of the system. In Section III the control

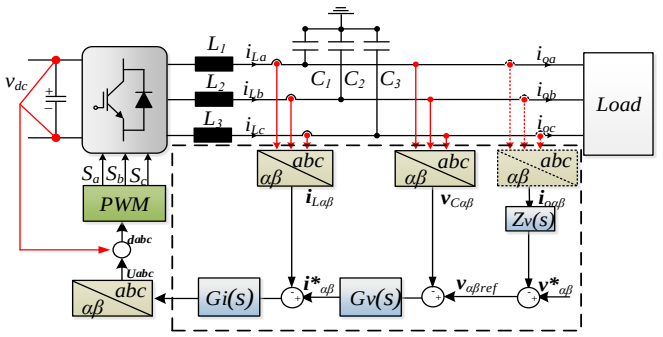

Fig. 2. General structure of the classical control for a voltage source converter (VSC) with an output LC filter.

algorithms and schemes for the comparative evaluation are discussed. Section IV gives the experimental results including discussion of the THD and efficiency calculation. Section V gives the conclusion of the paper.

II. System Model

1) Converter Model: The power circuit of the three phase 2L-VSC, as shown in Fig. 3, is considered, where the two switches in each leg operate in a complementary mode. The switching states can be represented by the switching signals S_a, S_b, and S_c, which are defined as follows:

$$S_a = \begin{cases} 1 \text{ if } S_1 \text{ on and } S_4 \text{ off} \\ 0 \text{ if } S_1 \text{ off and } S_4 \text{ on} \end{cases} \tag{1}$$

$$S_b = \begin{cases} 1 \text{ if } S_2 \text{ on and } S_5 \text{ off} \\ 0 \text{ if } S_2 \text{ off and } S_5 \text{ on} \end{cases} \tag{2}$$

$$S_c = \begin{cases} 1 \text{ if } S_3 \text{ on and } S_6 \text{ off} \\ 0 \text{ if } S_3 \text{ off and } S_6 \text{ on} \end{cases} \tag{3}$$

The filter inductance (L_1, L_2, L_3) equation can be expressed in the vectorial form as:

$$L\frac{\mathrm{d}I_f}{\mathrm{d}t} = V_i - V_c \tag{4}$$

where L is the filter inductance. The equation that describes the dynamic behaviour of the output voltage can be expressed mathematically as:

$$C\frac{\mathrm{d}V_c}{\mathrm{d}t} = I_f - I_o \tag{5}$$

where C is the filter capacitance (C_1, C_2, C_3). These equations can be rewritten in the state space model as:

$$\frac{\mathrm{d}X}{\mathrm{d}t} = AX + B_1V_i + B_2I_o \tag{6}$$

where,

$$X = \begin{bmatrix} I_f \\ V_c \end{bmatrix} \tag{7}$$

$$A = \begin{bmatrix} -R/L & -1/L \\ 1/C & 0 \end{bmatrix} \tag{8}$$

$$B_1 = \begin{bmatrix} 1/L \\ 0 \end{bmatrix} \tag{9}$$

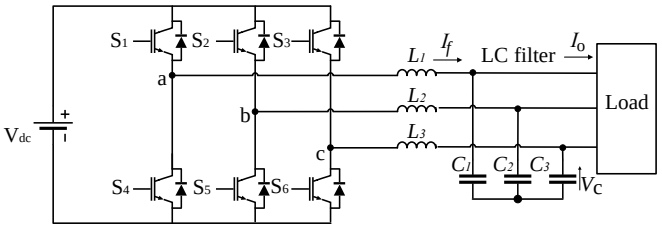

Fig. 3. Power circuit schematic for a stand-alone 2L-VSC.

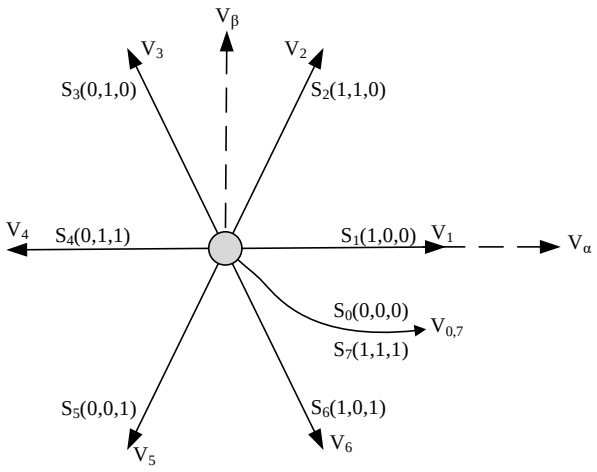

Fig. 4. Voltage vectors generated by the inverter.

$$B_2 = \begin{bmatrix} 0 \\ -1/C \end{bmatrix} \tag{10}$$

where I_f and V_c are the filter current and voltage respectively. I_o is the load current, which can be estimated or measured. V_i is the inverter voltage of the system and it has eight different voltage vectors as shown in Fig. 4.

A discrete model is obtained from (6) and it can be expressed as follows:

$$x\left(k+1\right) = A_q x\left(k\right) + B_q V_i\left(k\right) + B_{dq} I_o\left(k\right) \tag{11}$$

where,

$$A_q = exp^{AT_s} \tag{12}$$

$$B_q = \int_0^{T_s} exp^{A\tau} B_1 d\tau \tag{13}$$

$$B_{dq} = \int_0^{T_s} exp^{A\tau} B_2 d\tau \tag{14}$$

This model is used to calculate the prediction of filter voltages and currents for every possible input voltage. The selection of the optimal input voltage depends on the evaluation of CF [6]. Consequently, the new switching states are applied to the converter for the next sampling time.

2) Observer Model: Some considerations can be taken in order to build an appropriate observer. These considerations consist of assuming a certain dynamic behaviour of the load current. A simple consideration is to assume that the load current can be approximated as a constant, so its behaviour is described by the following equation:

$$\frac{\mathrm{d}I_o}{\mathrm{d}t} = 0 \tag{15}$$

After including this load-current model in the filter model, the system is described by the following state space equations:

$$\frac{\mathrm{d}}{\mathrm{d}t}\overbrace{\begin{bmatrix} I_f \\ V_c \\ I_o \end{bmatrix}}^{X} = \overbrace{\begin{bmatrix} 0 & -1/L & 0 \\ 1/C & 0 & -1/C \\ 0 & 0 & 0 \end{bmatrix}}^{A}\begin{bmatrix} I_f \\ V_c \\ I_o \end{bmatrix} + \overbrace{\begin{bmatrix} 1/L \\ 0 \\ 0 \end{bmatrix}}^{B} V_i \tag{16}$$

The output of this system are the two measured variables, the filter current and output voltage, and is defined by the following equation:

$$y = \overbrace{\begin{bmatrix} 1 & 0 & 0 \\ 0 & 1 & 0 \end{bmatrix}}^{C}\begin{bmatrix} I_f \\ V_c \\ I_o \end{bmatrix} \tag{17}$$

A full-order observer for the system can be used to estimate vector X. This is

$$\frac{\mathrm{d}\hat{X}}{\mathrm{d}t} = A\hat{X} + B_1 V_i + J(y - \hat{y}) \tag{18}$$

where $\hat{y} = CX$ and J is the observer gain. This equation can be rewritten as:

$$\frac{\mathrm{d}\hat{X}}{\mathrm{d}t} = A_{obs}\hat{X} + \begin{bmatrix} B & J \end{bmatrix}\begin{bmatrix} I_f \\ V_c \\ I_o \end{bmatrix} \tag{19}$$

where $A_{obs} = A - JC$. The output of the observer is the estimated load current

$$\hat{I}_o = \begin{bmatrix} 0 & 0 & 1 \end{bmatrix}\hat{X} \tag{20}$$

The matrix gain J defines the observer dynamics. As a design parameter, it must take into account the trade off between the bandwidth and noise rejection. In the next section, the control algorithms and control schemes, which are used in this work, will be discussed.

III. Control Algorithms and Schemes

As mentioned before, this work considers three algorithms with two different model predictive control algorithms and a CB-PWM control algorithm. In order to reduce the time taken to convert all the measurements into a digital form, two different predictive control schemes are used to assess the 2L-VSC performance. The first scheme is shown in Fig. 5(a), in which the full measurements of the filter current, load current, and the load voltage are used. Meanwhile, the scheme which is in Fig. 5(b), uses the filter current and load voltage to estimate the load current. Accordingly, the conversion time required by the control platform to embed the needed measurements into the algorithm is reduced. Additionally, each predictive control scheme applies two algorithms, where the first algorithm depends on predicting the voltage only in one sampling time of (T_s) as a primary objective of its CF. In the second algorithm, the tracking of the voltage and its derivative are considered in the optimization criterion. This could be obtained from the predicted currents, which are calculated from the discrete model of the 2L-VSC. Finally, the scheme, which is depicted in Fig. 5(c), uses a CB-PWM control algorithm. Generally, comparing the predictive control algorithms and their schemes with the CB-PWM control algorithm, provides somehow a classification for the predictive controller performance.

To sum up the above, each scheme applies two different predictive control algorithms in order to minimize the error and evaluate the proper actuation for controlling the 2L-VSC. Then, comparing these two predictive schemes with classical control algorithm using the scheme as demonstrated in Fig. 5(c) in terms of THDv, losses, and complexity of the control structure. In the next subsections, conventional control algorithm, improved control algorithm , and CB-PWM control algorithm will be discussed.

A. Conventional Model Predictive Control Algorithm

The conventional FCS-MPC algorithm is formulated in discrete time by allowing the voltage variable to change its value at discrete sampling instant. The future value of the state variable V is predicted for a prediction horizon N_1 by using the system model, which is discussed in Section II, and feed the measurements back at the K^{th} instant. The predictions are evaluated by the CF, which is described mathematically in (21), that defines the system control objective. In this case, the state variable V moves toward the reference trajectory V^*. The process of measuring new feed back variables, predicting new system behaviour, and optimizing the performance of the CF is repeated during each sampling interval.

$$g = (V^*_{c\alpha} - V^p_{c\alpha}(k+1))^2 + (V^*_{c\beta} - V^p_{c\beta}(k+1))^2 \tag{21}$$

B. Improved Model Predictive Control Algorithm

Using the CF in (21) may result in a satisfactory performance for the first order system but coupling between the state variables makes the performance somewhat unstable for second order systems. In the first order systems, the controlled variable can be directly regulated by the control input, allowing an instantaneous change of its derivative at a particular sampling instant. Capacitor voltage in the second order systems, which is used in this work, can only be regulated indirectly through the inductor current. Since this current cannot be changed instantaneously as well as the capacitor voltage cannot be changed instantaneously. Therefore, by involving only the capacitor voltage error as given in (21), the result is that the CF will have voltage trajectory pointing significantly away from the reference trajectory. These voltage deviations results in a high THDv in the measured voltage signal. In order to improve the 2L-VSC's capacitor voltage quality, a different FCS-MPC algorithm is used in this work. As

mentioned before, the inability to control the derivative of the capacitor voltage causes a high THD. Therefore, the regulator should track both the voltage reference and its derivative as described mathematically in (22). Further details can be found in [13, 15].

$$g = (V^*_{c\alpha} - V^p_{c\alpha}(k+1))^2 + (V^*_{c\beta} - V^p_{c\beta}(k+1))^2 + (\lambda_d * g_I) \tag{22}$$

$$g_I = (I_{f\alpha} - I_{o\alpha} + C\omega_{ref}(V^*_{c\beta}))^2 + (I_{f\beta} - I_{o\beta} + C\omega_{ref}(V^*_{c\alpha}))^2 \tag{23}$$

where the tracking of the voltage variables is already accomplished by the first two terms in Eqn. (22). The term g_I ensures that the voltage derivative tracks the reference and its importance is controlled by λ_d. Hence, the considered CF, as described in (22), can predict the voltage and control the current resulting in THDv improvement.

C. CB-PWM Control Algorithm

The conventional way of realizing overall 2L-VSC control structure is through organized linear loops and PWM. Therefore, compared with FCS-MPC, which is observing the past, present, and future values of the voltage variable, the classical control scheme deals with the past and present values of the variable. Basically, in order to adjust the magnitude and frequency of the fundamental frequency components for the power converter output voltage using CB-PWM, two important design factors (m_a and m_f) are utilized. m_a is adjusted by varying the amplitude of the modulating signals while retaining the fixed value of the carrier signals. m_f is modified by changing the carrier signal frequency while retaining the modulating signal frequency. The two indices are described as:

$$m_a = \frac{V_m}{V_{cr}} \tag{24}$$

$$m_f = \frac{f_{cr}}{f_m} \tag{25}$$

where V_m and V_{cr} are the peak values modulating and carrier signals, respectively. Also, f_{cr} and f_m are carrier and modulating signal frequencies, respectively.

The m_a is a factor ranging from zero to one, and the magnitude of the line-to-line voltages increases linearly with m_a. Moreover, the device switching frequency, in a 2L-VSC, is equal to the carrier frequency. However, voltage harmonics are concentrated around the switching frequency f_{sw} and its multiple. In CB-PWM, the maximum DC bus voltage utilization represents a narrow range of linearity. This can also be solved by the third harmonics injection PWM. However, classical control scheme, which is based on CB-PWM, takes the necessary control actions after the error has occurred as shown in Fig. 2. Contrarily, the FCS-MPC scheme implements preventive control actions even before a large voltage error arises. In addition, it eliminates the need of PI regulators and a modulation stage. Finally, the performance of the CB-PWM

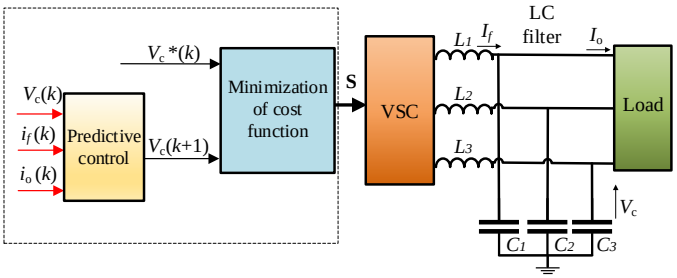

(a) Full measurements scheme for the conventional and improved FCS-MPC algorithm.

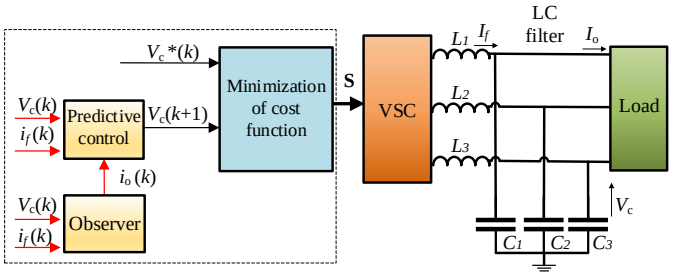

(b) Reduced measurements scheme for the conventional and improved FCS-MPC algorithm.

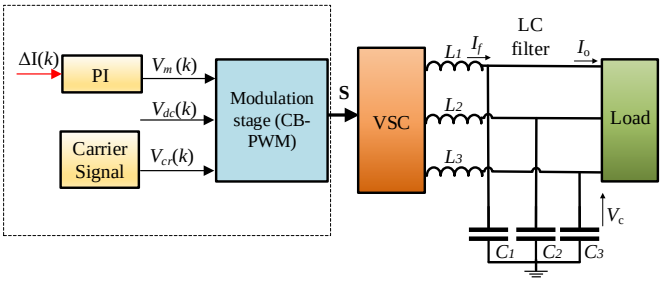

(c) CB-PWM control scheme for the classical control algorithm.

Fig. 5. Different control schemes. (a) Using full measurements; (b) using observer; and (c) using CB-PWM.

as well as the different FCS-MPC algorithms will be discussed in the experimental section.

IV. Experimental Analysis

The conventional, improved, and the CB-PWM control algorithms are tested experimentally using a SEMIKRON three-phase 2L-VSC with an output LC filter. The DC-link is fed by a power supply and the inverter is controlled using a dSpace DS1202 board. The parameters for the 2L-VSC are listed in Table I and Fig. 6 shows the experimental setup. The experimental validation is divided in twofold; a) the investigation of the THDv using the full measurements, observer, and the CB-PWM schemes. The THDv was investigated with 300 V DC-link and line to line output voltage which is equal to 173 V. In [13], where a higher DC-link (520 V) and AC output voltage (346) are tested in feeding both linear and non-linear load. And b) the investigation of the losses for the 2L-VCS using the parameters in Table I. In the losses

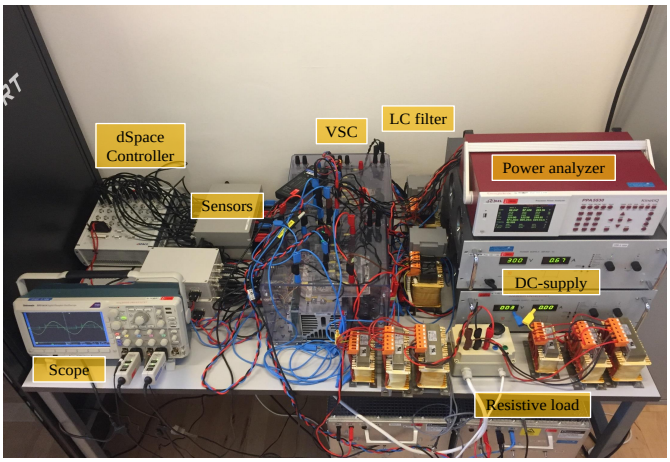

Fig. 6. Three-Phase two-level voltage source converter (VSC) setup.

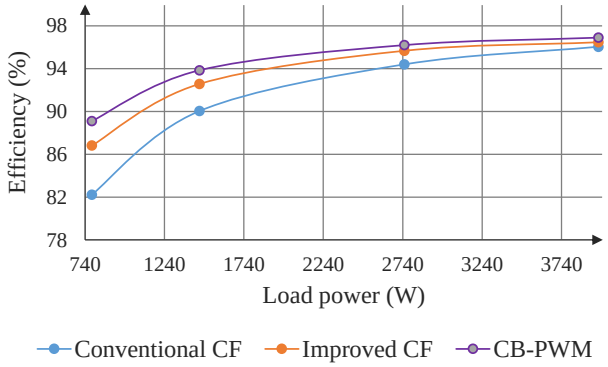

Fig. 7. Measured efficiency of the three-phase VSC using the three controling algorithms, feeding a linear load.

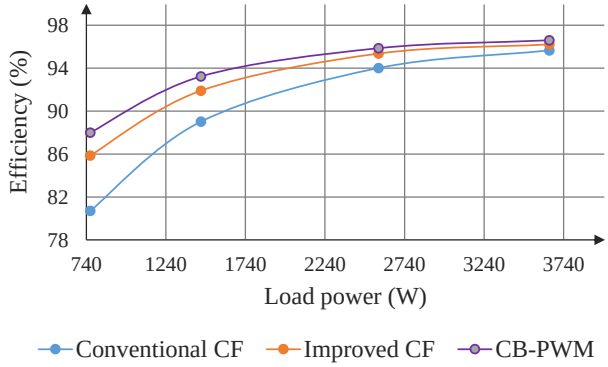

Fig. 8. Measured efficiency of the three-phase VSC using the three controling algorithms, feeding a non-linear load.

investigation, six sets of test has been carried out. The first and second tests consider the full measurements scheme using the conventional and improved predictive algorithms to feed a linear load. The third test is feeding a linear load where it is using the CB-PWM algorithm. Fourth and fifth tests consider the full measurements using the conventional and improved predictive algorithms where feeding a non-linear load. Finally, last test is feeding a non-linear load where it is using the CB-PWM algorithm. It is worth to mention that the CB-PWM is an open-loop control and in the future work the closed loop-control will be considered.

TABLE I
PARAMETERS OF THE THREE-PHASE VOLTAGE SOURCE CONVERTER (VSC).

Quantity	**Value**
DC link voltage V_{dc}	700 V
Filter inductance L (L_1,L_2,L_3)	2.4 mH
Filter capacitor C (C_1,C_2,C_3)	13 μF
Resistive load R	57-460 Ω
Non-linear load R and $Diodebridge$	57-460 Ω
Sampling time T_s	25 μS
Average switching frequency f_{sw}	6000$\pm$200Hz

1) Linear load: The line-to-line load voltage is shown for the both algorithms in Fig. 9(a) and Fig. 9(b), where these tests were done by using the full measurements of the 2L-VSC as shown in the Fig. 5(a). The second test has been done in order to evaluate the performance of both algorithms using an observer, which is used to estimate the load current (I_o) and apply it to the conventional and improved algorithms. Based on that, the time required by the control platform for the analog to digital conversion is reduced due to reducing the number of analog to digital channels. Knowing that, using an observer to estimate the current gave similar results in terms of THDv as using the full measurements scheme. The line-to-line load voltage is shown in the Fig. 9(c) and Fig. 9(d) for both algorithms using the observer. Note that the fundamental voltage magnitude and the THDv calculations are reported in the captions of the four experimental figures. It is worth to mention that the THDv for the CB-PWM equal to 0.98%. On the other hand, a loss evaluation for the 2L-VSC has been done by using the three algorithms. The power loss has been measured using the power analyser KinetiQ PPA5530. Fig. 7 shows the measured efficiency of the 2L-VSC using the conventional, improved, and CB-PWM algorithms. It can be seen that the CB-PWM has the best efficiency and also the improved FCS-MPC has a lower efficiency. Fig. 10(a), shows an example of the output voltage and current using the conventional algorithm for low load operation. Fig. 11(a) shows an example of the output voltage and current using the conventional algorithm for full load operation. Consecutively, Figs. 10(b) and 11(b) show the the output voltage and current using the improved algorithm for low and full load operation respectively.

2) Non-linear load: A load is considered as a non-linear load if its impedance changes with the applied voltage. The change in the impedance means that the current drawn by the non-linear load will not be sinusoidal even it is connected to a sinusoidal voltage. Nowadays, harmonic problems are common not only in industrial applications but also in commercial buildings as well. For instance, the new power conversion technologies such as the switched-mode power supply (SMPS),

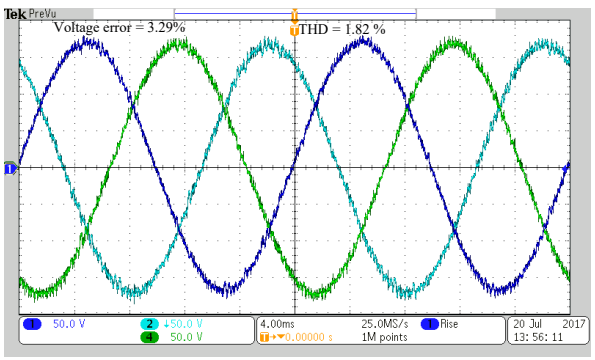

(a) Conventional FCS-MPC algorithm using the full measurements scheme.

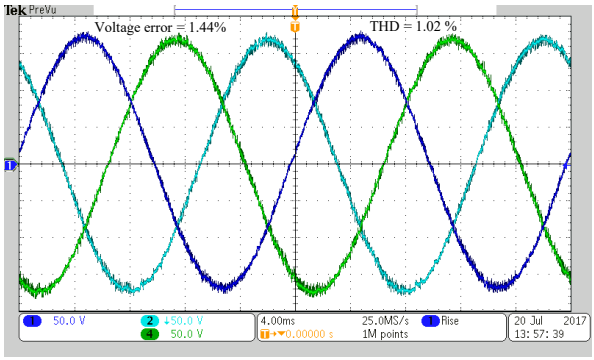

(b) Improved FCS-MPC algorithm using the full measurements scheme.

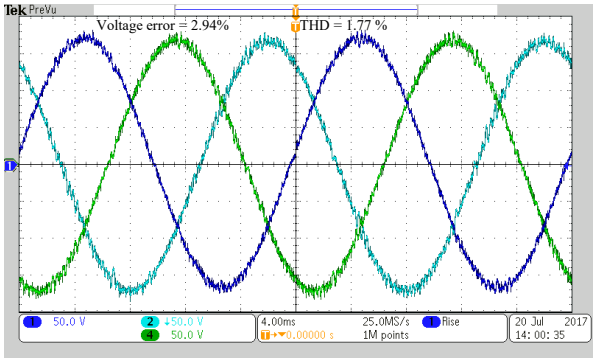

(c) Conventional FCS-MPC algorithm using the observer scheme.

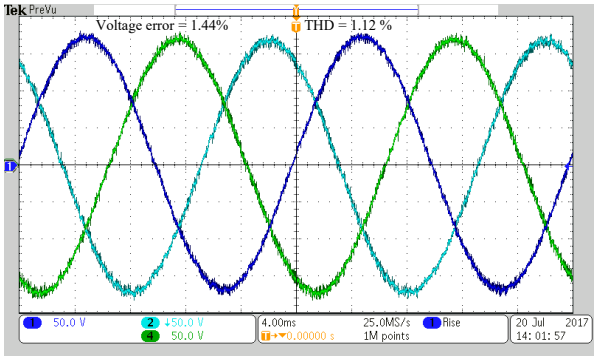

(d) Improved FCS-MPC algorithm using the observer measurements scheme.

Fig. 9. Line-to-line output voltage using different MPC schemes and algorithms. (a) The conventional algorithm using full measurements scheme, where the THD = 1.82 % and the fundamental voltage amplitude = 167.5 V; (b) the improved algorithm using full measurements scheme, where the THD = 1.02 % and the fundamental voltage amplitude = 170.5 V; (c) the conventional algorithm using observer scheme, where the THD = 1.77 % and the fundamental voltage amplitude = 167.9 V; and (d) the improved algorithm using observer scheme, where the THD = 1.12 % and the fundamental voltage amplitude = 170.5 V.

which can be found in every power electronic device is an excellent power supply, but it has a highly non-linear load. This subsection discuss the behaviour of a 2L-VSC, where it is connected to a non-linear load, using the different three control schemes. As discussed in the linear load subsection, Fig. 8 shows the measured efficiency of the 2L-VSC using the conventional, improved, and CB-PWM algorithms. It can be seen that the CB-PWM has the best efficiency among the three methods and also the improved FCS-MPC has a lower efficiency. Fig. 10(c), shows an example of the output voltage and current using the conventional algorithm for low load operation. Fig. 11(c) shows an example of the output voltage and current using the conventional algorithm for full load operation. Consecutively, Figs. 10(d) and 11(d) show the output voltage and current using the improved algorithm for low and full load operation respectively.

V. Conclusion

In this paper an assessment of the 2L-VSC performance in steady state operation has been introduced. Three different control schemes have been applied to the 2L-VSC, which are feeding a linear load and non-linear load. One scheme is measuring all variables such as filter currents, load currents, and the load voltages. Meanwhile, the other scheme estimates the load current and measures both the filter current and load voltage. Each scheme considers two algorithms: the conventional and the improved algorithm in order to evaluate the cost function. The third scheme applies the CB-PWM control algorithm and compares it with both predictive controller schemes. In that context, the evaluation of the losses for the 2L-VSC is presented using the three algorithms. Moreover, the THDv for the improved CF is significantly reduced comparing to the conventional CF and resulting in reducing the percentage of total losses, which can improve the overall efficiency. Experimental validation for the schemes and algorithms was conducted up to 4 kW output power. The results showed that the improved predicted control has almost the same performance such as the CB-PWM in the power loss. The results also show that the predictive schemes using the observer gave a similar performance as using the full measurements scheme. This significantly reduce the total conversion time, which is required by the control platform. Finally, it can be concluded that a comparable performance for the 2L-VSC is achieved by using the conventional FCS-MPC, Improved FCS-MPC, and CB-PWM algorithms.

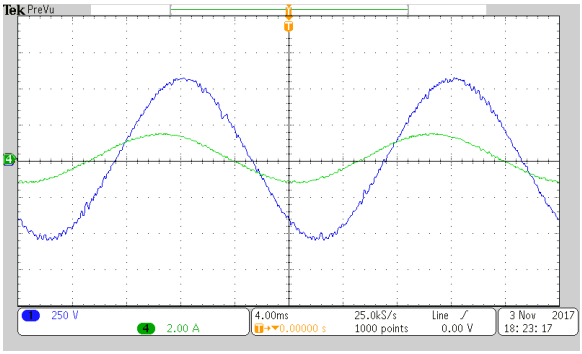

(a) Conventional FCS-MPC algorithm using the full measurements scheme.

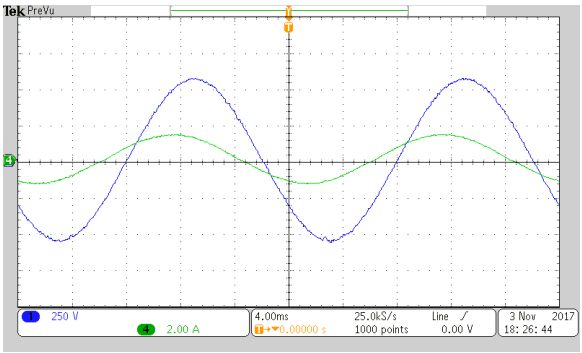

(b) Improved FCS-MPC algorithm using the full measurements scheme.

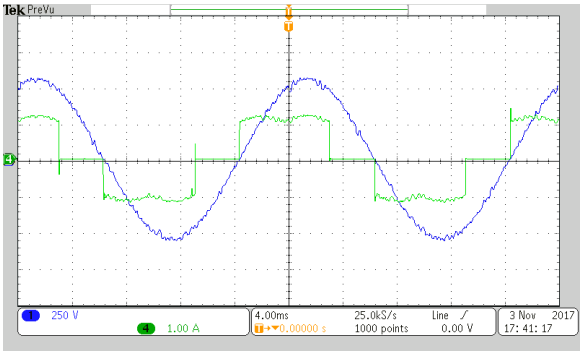

(c) Conventional FCS-MPC algorithm using the full measurements scheme.

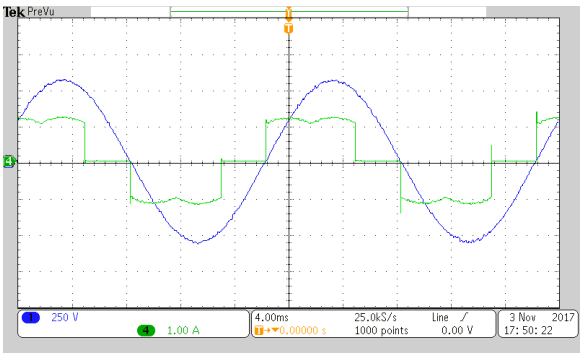

(d) Improved FCS-MPC algorithm using the full measurements scheme.

Fig. 10. Line-to-line output voltage using different algorithms, where the test has been done for a low power level. (a) The conventional algorithm using full measurements scheme, where the test has been done for a linear load. (b) the improved algorithm using full measurements scheme, where the test has been done for a linear load. (c) The conventional algorithm using full measurements scheme, where the test has been done for a non-linear load; (d) the improved algorithm using full measurements scheme, where test has been done for a non-linear load.

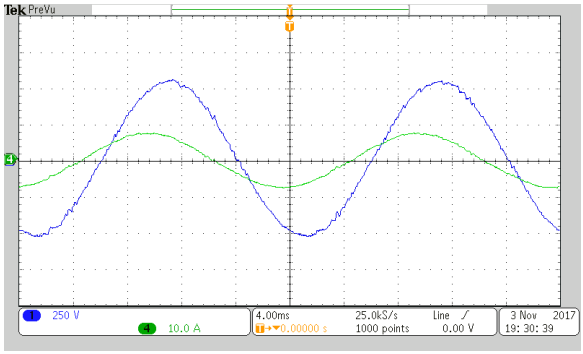

(a) Conventional FCS-MPC algorithm using the full measurements scheme.

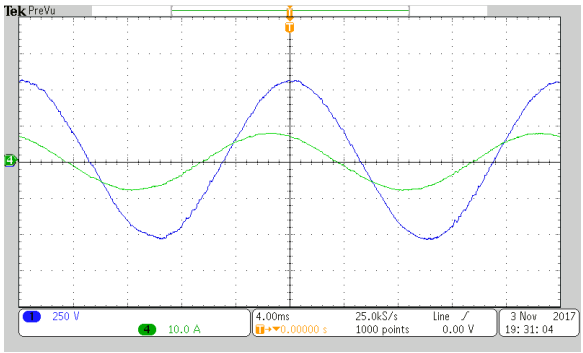

(b) Improved FCS-MPC algorithm using the full measurements scheme.

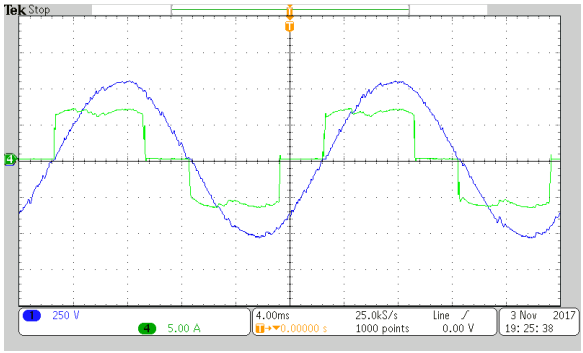

(c) Conventional FCS-MPC algorithm using the full measurements scheme.

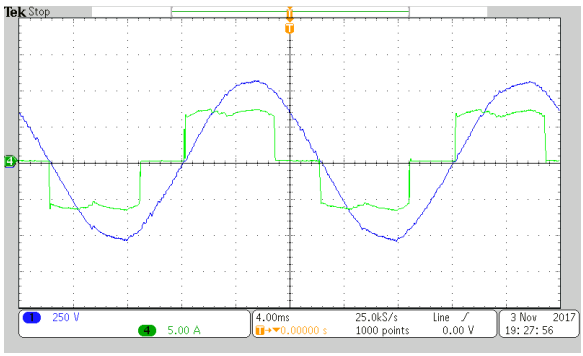

(d) Improved FCS-MPC algorithm using the full measurements scheme.

Fig. 11. Line-to-line output voltage using different algorithms, where the test has been done for a high power level, 4kW. (a) The conventional algorithm using full measurements scheme, where the test has been done for a linear load. (b) the improved algorithm using full measurements scheme, where the test has been done for a linear load. (c) The conventional algorithm using full measurements scheme, where the test has been done for a non-linear load; (d) the improved algorithm using full measurements scheme, where the test has been done for a non-linear load.

References

[1] H. Han, X. Hou, J. Yang, J. Wu, M. Su, and J. M. Guerrero, "Review of power sharing control strategies for islanding operation of ac microgrids," *IEEE Trans. on Smart Grid*, vol. 7, pp. 200–215, Jan 2016.

[2] A. Abdelhakim, P. Mattavelli, V. Boscaino, and G. Lullo, "Decoupled control scheme of grid-connected split-source inverters," *IEEE Trans. on Ind. Electron.*, vol. 64, pp. 6202–6211, Aug 2017.

[3] F. Blaabjerg, K. Ma, and Y. Yang, "Power electronics - the key technology for renewable energy systems," in *2014 Ninth International Conference on Ecological Vehicles and Renewable Energies (EVER)*, pp. 1–11, March 2014.

[4] F. Blaabjerg, Y. Yang, D. Yang, and X. Wang, "Distributed power-generation systems and protection," *Proc. of the IEEE*, vol. 105, pp. 1311–1331, July 2017.

[5] A. Abdelhakim, P. Mattavelli, D. Yang, and F. Blaabjerg, "Coupled-inductor-based dc current measurement technique for transformerless grid-tied inverters," *IEEE Trans. on Power Electron.*, vol. 33, pp. 18–23, Jan 2018.

[6] J. Rodriguez and P. C. Estay, *Predictive control of power converters and electrical drives*. Chichester West Sussex UK: Wiley-IEEE Press, 2012.

[7] P. Mattavelli, "An improved deadbeat control for ups using disturbance observers," *IEEE Trans. Ind. Electron*, vol. 52, pp. 206–212, Feb 2005.

[8] P. C. Loh and D. G. Holmes, "Analysis of multiloop control strategies for lc/cl/lcl-filtered voltage-source and current-source inverters," *IEEE Trans. Ind. Appl.*, vol. 41, pp. 644–654, Mar 2005.

[9] S. Buso, S. Fasolo, and P. Mattavelli, "Uninterruptible power supply multiloop control employing digital predictive voltage and current regulators," *IEEE Trans. Ind. Appl.*, vol. 37, pp. 1846–1854, Nov 2001.

[10] R. Aliaga, J. Munoz, F. Cadena, and J. Guzman, "Voltage source converter based statcom with predictive and fuzzy control," in *Proc. of IEEE International Conference on Automatica (ICA-ACCA)*, pp. 1–7, Oct 2016.

[11] J. Rodriguez, P. Cortes, R. Kennel, and M. P. Kazrnierkowski, "Model predictive control – a simple and powerful method to control power converters," in *Proc. of IEEE 6th International Power Electronics and Motion Control Conference*, pp. 41–49, May 2009.

[12] P. Cortes, G. Ortiz, J. I. Yuz, J. Rodriguez, S. Vazquez, and L. G. Franquelo, "Model predictive control of an inverter with output lc filter for ups applications," *IEEE Trans. Ind. Electron.*, vol. 56, pp. 1875–1883, June 2009.

[13] T. Dragicevic, M. Alhasheem, M.Lu, and F. Blaabjerg, "Improved model predictive control for high voltage quality in ups applications," in *Proc. of 2017 IEEE Energy Conversion Congress and Exposition (ECCE), Cincinnati, OH*.

[14] M. Kazmierkowski, R. Krishnan, and F. Blaabjerg, *Control in Power Electronics: selected problems*. United States: Academic Press, 2002.

[15] T. Dragicevic, "Model predictive control of power converters for robust and fast operation of ac microgrids," *IEEE Trans. on Power Electron.*, vol. PP, no. 99, pp. 1–1, 2017.